







Climatological Features of the Vento Norte Phenomenon in the Extreme South of Brazil

Características Climatológicas do Fenômeno Vento Norte no Extremo Sul do Brasil

Cinara Ewerling da Rosa¹ , Michel Stefanello² , Douglas Stefanello Facco³ ,
Débora Regina Roberti² , Fábio Diniz Rossi⁴  & Gervásio Annes Degrazia² 

¹Instituto Federal Farroupilha, Campus São Vicente do Sul, São Vicente do Sul, RS, Brasil

²Universidade Federal de Santa Maria, Departamento de Física, Santa Maria, RS, Brasil

³Universidade Federal do Rio Grande do Sul, Centro de Investigação em Detecção Remota e Meteorologia, Porto Alegre, RS, Brasil

⁴Instituto Federal Farroupilha, Campus Alegrete, Alegrete, RS, Brasil

E-mails: cinara.rosa@iffarroupilha.edu.br; michelstefanello@gmail.com; douglas.s.facco@gmail.com; debora@ufsm.br;

fabio.rossi@iffarroupilha.edu.br; gervasio.degrazia@gmail.com

Corresponding author: Cinara Ewerling da Rosa; cinara.rosa@iffarroupilha.edu.br

Abstract

Downslope windstorm known as Vento Norte (VNOR; Portuguese for “North Wind”) is a common phenomenon that occurs in southern Brazil during the winter season. Hence, this study attempted to investigate the climatological characteristics of VNOR using seventeen years (2004–2020) of hourly observations collected at seven meteorological stations distributed over the central region of Rio Grande do Sul State. The VNOR windstorm episodes are identified by intense wind gusts and warm air advection from the northern direction. They were selected from the data set obtained during the winter in the city of Santa Maria (SM). Statistical analysis showed that the detected VNOR events were characterized by mean wind gusts $\approx 15 \text{ m.s}^{-1}$, mean wind direction of 350° and mean air temperature of 27°C . Average duration of the events was about 9 h, with the longest event lasting 21 h. Characteristics and effects of this phenomenon were compared with those in other locations (meridional and zonal sections). Average values of wind gusts from the northern direction presented a significant increase of $\approx 200\%$ for the winter period in SM. Nonetheless, a less significant increase in wind gusts was recorded in the meridional (28%) and zonal (41%) sections away from SM. The central location of SM has favorable topographic characteristics for this amplification, with a sharp altitude difference caused by the plateau-plain interface of $\approx 300 \text{ m}$. Our findings showed that the VNOR phenomenon mainly affects the climate of the southern region of Brazil, with a local amplification in the city of SM.

Keywords: Downslope winds; Regional advection; Local topography

Resumo

A tempestade de vento conhecida como Vento Norte (VNOR) é um fenômeno comum que ocorre no sul do Brasil durante o inverno. Assim, este estudo buscou investigar as características climatológicas do VNOR utilizando dezessete anos (2004-2020) de observações horárias coletadas em sete estações meteorológicas distribuídas na região central do Rio Grande do Sul. Os episódios de VNOR, identificados por rajadas de vento intensas e advecção de ar quente da direção norte, foram selecionados a partir do conjunto de dados obtidos durante o inverno na cidade de Santa Maria (SM). A análise estatística realizada mostrou que os eventos de VNOR detectados foram caracterizados por rajadas de vento médias $\approx 15 \text{ m.s}^{-1}$, direção média do vento de 350° e temperatura média do ar de 27°C . A duração média dos eventos foi de cerca de 9 horas, sendo que o evento mais longo durou 21 horas. As características e efeitos deste fenômeno foram comparados com os de outras localidades (seções meridional e zonal). Os valores médios de rajadas de vento da direção norte apresentaram um aumento significativo de $\approx 200\%$ para o período de inverno em SM. Por outro lado, registou-se um aumento menos significativo das rajadas de vento nas seções meridional (28%) e zonal (41%) afastadas de SM. A localização central de SM apresenta características topográficas favoráveis a esta amplificação, com uma acentuada diferença de altitude causada pela interface planalto-planície de $\approx 300 \text{ m}$. O estudo mostrou que o fenômeno VNOR afeta principalmente o clima da região sul do Brasil, com uma amplificação local na cidade de SM.

Palavras-chave: Ventos descendentes; Advecção regional; Topografia local

Received: 26 May 2022; Accepted: 07 November 2022

Anu. Inst. Geociênc., 2023;46:52599

DOI: https://doi.org/10.11137/1982-3908_2023_46_52599 1

1 Introduction

Various topographic features of the Earth's surface influence the patterns of meteorological airflows acting on the planetary boundary layer (PBL) at different scales. In particular, mesoscale geophysical flows induced by sloping topography influence climatological and turbulent patterns in different regions of the planet (Abatzoglou et al. 2021; Arbage et al. 2008; da Rosa et al. 2021b, 2022; Stefanello et al. 2020; Wang et al. 2016). In this aspect, various authors have reported some well-known phenomena associated with these types of flow, including the Chinook wind in the east of the Rocky Mountains and northwestern Canada (MacDonald, Pomeroy & Essery 2018; Math 1934), the Foehn wind in the Austrian Alps (Richner & Hächler 2013; Würsch & Sprenger 2015), the Bora wind, Spitsbergen and Yuzhak (in Pevek), in the Russian Arctic (Efimov & Komarovskaya 2018; Láska, Chládová & Hošek 2017; Moore 2013; Samuelsen & Graversen 2019; Shestakova & Moiseenko 2018; Shestakova, Toropov & Matveeva 2020), the Santa Ana wind in southern California (Abatzoglou, Barbero & Nauslar 2013; Mass & Ovens 2019; Raphael 2003; Smith, Hatchett, & Kaplan 2018) and the Zonda wind in the Andes Mountains of central-western Argentina (Norte 2015; Otero & Araneo 2021). These phenomena are characterized by well-defined periods and specific weather patterns. Despite their individuality, these events combine strong winds with extreme magnitudes of temperatures and relative humidity.

There is currently great interest in understanding downslope windstorms as they play an important role, such as in the vertical evolution of the PBL structure (Jensen et al. 2017; Lehner et al. 2015; Lothon et al. 2014; Román-Cascón et al. 2015; Sun et al. 2006; Whiteman 1982), the formation of fog and ice (Hang et al. 2016), their influence on the exchange of heat, humidity, CO₂ and other scalars between the surface and the atmosphere (Arrillaga et al. 2019) and the regional atmospheric dispersion of pollutants (Li et al. 2018). Moreover, a better knowledge of downslope flows is important not only in the area of meteorology but also in various fields such as agriculture, transport, civil defense, livestock, construction and other human activities (Cooke, Rose & Becker 2000; Cruz et al. 2020; Heldwein et al. 2003; Sartori 2016).

The city of Santa Maria (SM) is located in the central region of Rio Grande do Sul State (RS) in southern Brazil and is characterized by a particular topography. The steep edge of the Brazilian Meridional Plateau, which borders

SM, is oriented approximately in an east-west direction with an elevation slope of 300 m. Among the many significant weather patterns affecting this region, the occurrence of strong northerly gusts, accompanied by an abrupt increase in temperature and a drop in relative humidity, is a typical pattern known as “Vento Norte” (VNOR; Portuguese for “North Wind”; Arbage et al. 2008; da Rosa et al. 2021a, 2021b, 2022; Sartori 2003; Stefanello et al. 2020). This phenomenon often occurs in the winter and is associated with the prefrontal systems. The large-scale synoptic environmental conditions responsible for developing the VNOR flow can be associated with cyclogenesis in the La Plata Basin and a high-pressure system near the coast of southern Brazil, as described by Stefanello et al. (2020).

Although the VNOR windstorm is a frequent phenomenon widely known in southern Brazil and with significant impacts on society, it has been little studied in the literature (Arbage et al. 2008; da Rosa et al. 2021a, 2021b, 2022; Sartori 2003; Stefanello et al. 2020). The above mentioned studies have contributed to the systematic understanding of the VNOR phenomenon in the central region of RS. However, its characterization is challenging from the climatological and micrometeorological points of view and in terms of its relationship to large-scale synoptic features such as the Pacific Decadal Oscillation and the El Niño-Southern Oscillation.

Given the above, this study aims to perform a temporal statistical analysis of hourly atmospheric observations in SM, covering the winter period from 2004 to 2020, in order to obtain a local climatology of the VNOR windstorm phenomenon. In addition, a comparison of the atmospheric anomaly patterns during the VNOR development in large a part of RS will also be addressed.

The paper is structured as follows: Section 2 introduces the experimental site and the approach used to detect VNOR episodes and Section 3 describes the climatological analysis of VNOR; this section also compares the main atmospheric variables for the winter periods with VNOR and No-VNOR for seven weather stations in RS. Lastly, Section 4 provides the conclusions.

2 Methodology and Data

Geographical location of the meteorological data used in this study refers to South America, east of the Andes. More specifically, data were acquired in southern Brazil, in the central region of RS between latitudes 28°36' and 30°32'S and longitudes 52°22' and 55°31'W (Figure 1A).

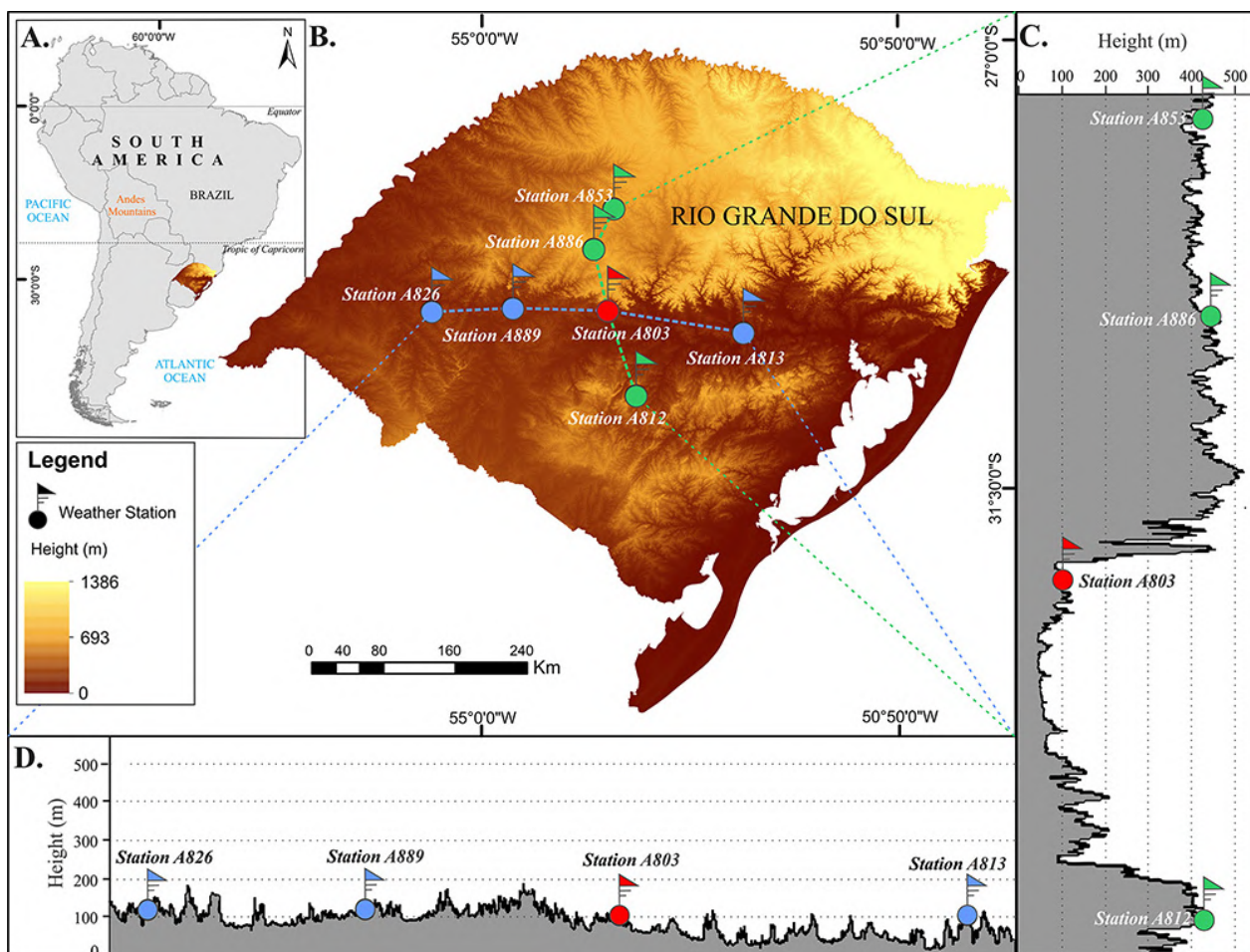


Figure 1 A. Location of the Rio Grande do Sul state (RS) in relation to South America; B. Terrain elevation of RS (in m; see color convention); C. Cross-section along the north-south line indicated on panel B; D. Cross-section along the west-east line indicated on panel B. Colored circles indicate the location of the automated weather stations. Data source: United States Geological Survey (USGS, 2022). Shuttle Radar Topography Mission (SRTM) data spatialized in the geographic information system (GIS) ArcGIS 10.6.1. WGS84 cartographic projection system.

The observations were carried out in the central region of the state, in the city of SM (S_c ; Figure 1B [Station A803 - red]). Starting from Section S_c , the study area is divided into two sections: a meridional section (S_m ; Figure 1C [green]), which includes a network of weather stations from the North to the South, passing through the cities of Cruz Alta (CRA; Station A853), Tupanciretã (TUP; Station A886) and Caçapava do Sul (CAP; Station A812). And a zonal section (S_z ; Figure 1D [blue]), oriented approximately from the West to the East and passing through the cities of Alegrete (ALG; Station A826), São Vicente do Sul (SVS; Station A889) and Rio Pardo (RPA; Station A813).

The specifications of the measurement locations and INMET operational automated weather stations installed in each city are listed in Table 1. Hourly meteorological data

used in this study were obtained from INMET stations 10 m above the ground for velocity and 2 m for temperature measurements for seventeen consecutive winters between 2004 and 2020 (from 21/06 to 21/09).

The study region has particular geographical features and a marked topography contrast. The land surface consists of a plateau relive and a ridge extending from the East to the West. In this environment, the topography of SM is characterized by a steep slope with an altitude difference of about 400 m, which marks the abrupt transition between the high plateau in the North and the depression in the South. The cities in Section S_z have a slight elevation change of about 110m compared to SM and follow the edge of the central depression. In contrast, the cities in Section S_m are located in higher regions than section S_c .

Table 1 Geographical coordinates and terrain elevation of INMET's automated weather stations.

Section	Station	City	Latitude (S)	Longitude (W)	Altitude (m)
S _c	A803	Santa Maria (SM)	29°43'29.27"	53°43'13.67"	103.10
S _m	A853	Cruz Alta (CRA)	28°36'12.38"	53°40'13.95"	426.69
S _m	A886	Tupanciretã (TUP)	29°05'21.77"	53°49'13.94"	462.00
S _m	A812	Caçapava do Sul (CAP)	30°32'43.14"	53°28'13.38"	420.82
S _z	A826	Alegrete (ALG)	29°42'32.70"	55°31'13.75"	120.88
S _z	A889	São Vicente do Sul (SVS)	29°42'07.60"	54°39'13.55"	134.00
S _z	A813	Rio Pardo (RPA)	29°52'19.61"	52°55'13.13"	106.99

2.1 Definition VNOR in Section Sc

During the winter months, atmospheric variables in SM show a climatological pattern characterized by average temperatures varying from -2 to 35 °C and average wind gusts of 5 m.s^{-1} ; the preferential wind direction in this region is predominantly from the East and the Southeast. The average atmospheric pressure and relative humidity values during these periods are 1007 hPa and 82%, respectively.

As illustrated in Figure 2, a pattern characterized by strong wind gusts from the northern quadrant significantly alters the flow regime in winter. These strong gusts are accompanied by temperatures much higher than the climatological normal for winter; such characteristics are commonly referred to as the VNOR phenomenon (Arbage et al. 2008; da Rosa et al. 2021b, 2022; Sartori 2016; Stefanello et al. 2020). The criteria used to identify VNOR episodes correspond to those suggested by da Rosa et al. (2022) and Nascimento and Chamis (2012). According to these authors, the detailed criteria are:

I. **Wind direction:** in the northern quadrant ranging between 300° (West-Northwest) and 30° (North-Northeast);

II. **Wind velocity:** gusts greater than 11 m.s^{-1} ;

III. **Surface air temperature:** maximum air temperature with values above the 90% percentile (90P) of the respective time and month during at least half of the VNOR event;

IV. **Duration:** all the above conditions are met for at least four consecutive hours.

The above criteria are applied to INMET's hourly atmospheric observations presented in the previous section for the SM site. Figure 2 summarizes these criteria in relation to data collected for seventeen consecutive winters (2004–2020), highlighting the presence of VNOR windstorms indicated by purple color dots. It is not surprising that the strongest wind gusts during this period are related to the northerly wind direction, as has been documented elsewhere (da Rosa et al. 2022; Stefanello et al. 2020).

Heat Wave episodes in southern Brazil are identified using the method proposed by dos Reis, Boiaski and Ferraz (2019). This method defines a heat wave as an interval of over four days in which the daily maximum temperature is above the percentile (P90) of daily temperature anomalies; the authors determined the P90 for the 1981–2010 reference period.

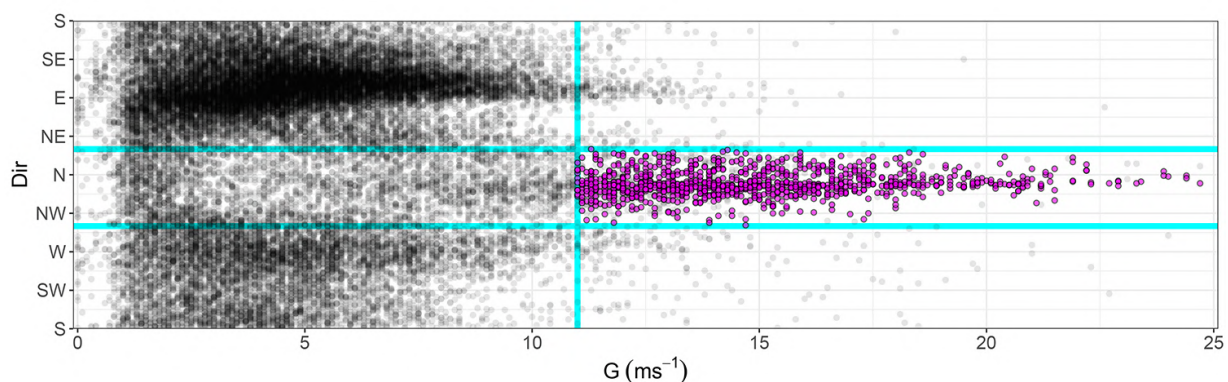


Figure 2 Relationship between wind direction and magnitudes of the wind gust (in m.s^{-1}) for SM. Conditions that meet the VNOR criteria (I), (II) and (III) are shown in purple. Cyan lines correspond to the limit wind direction and wind gust criteria for VNOR events.

3 Results and Discussion

3.1 VNOR Characteristic in Section Sc

Previous studies have systematically documented the presence of VNOR windstorms during the winter months in central RS by analyzing local and regional atmospheric patterns and identifying them globally using reanalysis data (Abatzoglou et al. 2021; da Rosa et al. 2022; Stefanello et al. 2020). Intense warm air advection from a northerly direction commonly affects local meteorological conditions. Here, this downslope windstorm is studied using the anomaly of the main atmospheric variables for the winter months in the 2004–2020 period. The conditional probability function (CPF) is an effective method for obtaining information on the high percentile of atmospheric variables that can help identify unseasonable patterns, such as the VNOR windstorm (Ashbaugh, Malm & Sadeh 1985). The CPF can be expressed by the following Equation 1 (Iratxe & Carslaw 2014):

$$CPF_{\Delta\theta} = \frac{m_{\Delta\theta, C > x}}{n_{\Delta\theta}} \quad (1)$$

where $m_{\Delta\theta}$ is the number of measurements in the wind quadrant θ whose values of a given atmospheric quantity C are greater than or equal to a threshold x (90P) and $n_{\Delta\theta}$ is the total number of measurements from the wind quadrant $\Delta\theta$.

The probability of measuring anomalies of maximum temperature, relative humidity and atmospheric

pressure above 90P with wind direction and gusts is shown in Figure 3. In Figures 3A and 3B, the highest probability ($\geq 50\%$) of maximum temperature and relative humidity values above 90P ($T_{\max} \geq 25^\circ\text{C}$; $RH_{\max} \leq 54\%$) is associated with a wind gust above $9\text{ m}\cdot\text{s}^{-1}$. Moreover, the wind direction is well consolidated from the northern quadrant ($\geq 60\%$), ranging between 300 and 30° . In addition, the probability of air pressure anomalies ($P_{\max} \leq 999\text{ hPa}$) is also observed in the pressure field but is less pronounced than the RH_{\max} and T_{\max} anomalies (Figure 3C). Therefore, the large probabilities of anomalies in atmospheric variables during the winter are associated with a range of wind directions from the northern regions and strong wind gusts. These patterns and particular features of the atmospheric variables reveal the presence and manifestation of the VNOR windstorm in central RS. Moreover, it can be seen that there are T_{\max} and P_{\max} anomalies in the southwestern quadrant but not in RH_{\max} . It is important to note that this last variable is not included in the criteria for detecting VNOR (Section 2.1). Nonetheless, it may help identify and characterize the phenomenon since T_{\max} , P_{\max} and RH_{\max} have significant anomalies in the northern quadrant.

120 VNOR episodes were identified by applying this discussed VNOR detection method (Section 2.1), spanning about 1050 h, with a mean duration of each event of about 9 h. Such events are characterized by average gusts (G) of $\approx 15\text{ m}\cdot\text{s}^{-1}$, an average wind direction (Dir) of $\approx 350^\circ$ and an air temperature (T_{\max}) of $\approx 27^\circ\text{C}$.

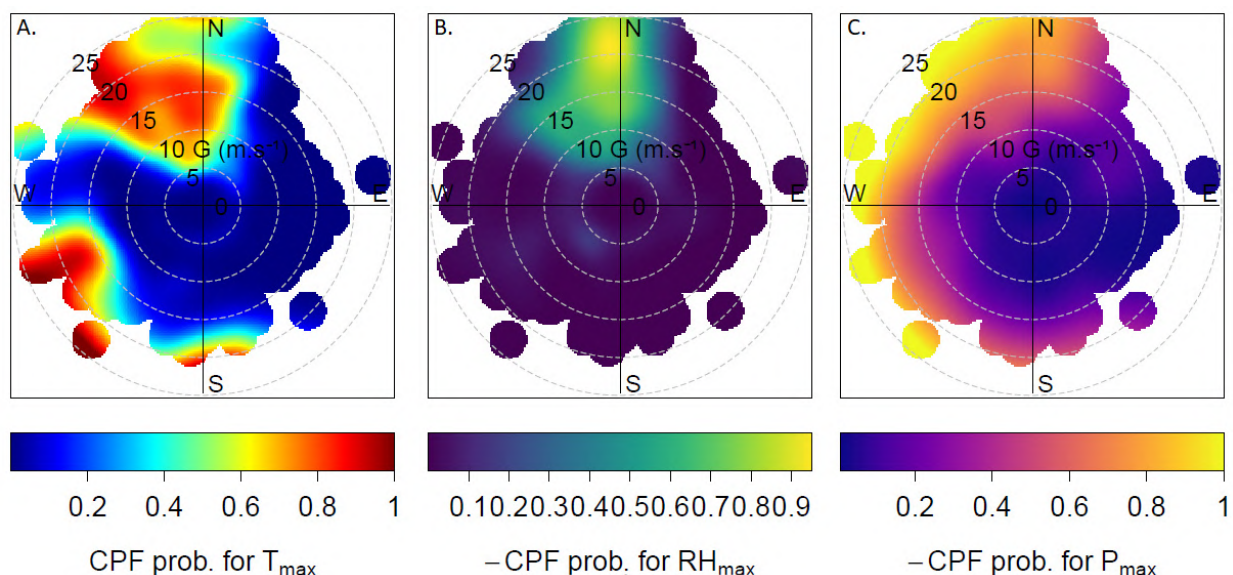


Figure 3 Polar plot showing the conditional probability function of the anomalies of: A. T_{\max} ; B. RH_{\max} ; C. P_{\max} . The radial axis shows wind gust intervals and the colors of the probability of reaching $> 90\text{P}$ values. This is shown for each bin composed by wind direction and wind gust (in $\text{m}\cdot\text{s}^{-1}$) in Section S_c . The plot was produced in R with the Openair package (Carslaw & Ropkins 2012).

Figure 4A shows the time series of total annual hours (duration) of VNOR in seventeen consecutive winters (2004–2020). The years 2006 and 2007 had the highest accumulations of VNOR hours, with 2007 having the highest average duration of VNOR cases (average lifetime of each event of 13 h). In addition, 2004, 2005, 2010, 2013, 2014, 2015 and 2017 had episodes of heat waves that occurred when VNOR was detected and 2015 recorded this overlap of events in over 56% of recorded VNOR hours. This year also recorded the largest event with 21 h. The year 2015 is associated with intense El Niño phenomenon (Pereira, Reboita & Ambrizzi 2017).

Figure 4B shows the mean annual frequency of events over the 16-year climatology, which was about seven events per year (Figure 4B, cyan line). The most active year was 2006, with 12 events; the most inactive years were 2008 and 2009, with only four events recorded. Note that 2018 had only one event, but this fact is related to the data gaps in which 2018 had over 80% of hours disregarded in the analysis, as well as 2011, 2012 and 2020 (Figure 4B, blue dots) with outages of more than one month. In the winter period, July

and August showed the highest frequency of VNOR events, while September they were much less frequent.

3.2 VNOR Characteristics in the Sections S_c , S_m and S_z

The characteristics and effects of the VNOR windstorm observed in SM were compared with those measured in different regions of southern Brazil (Figure 5). As shown in Figure 5, the probability density functions (p.d.f.) of temperature, wind gust and direction, air pressure and relative humidity are bimodal in Sections S_c , S_z and S_m . In this figure, there is a maximum in the p.d.f. associated with the VNOR cases and another maximum associated with the non-VNOR cases. The results showed that two different patterns characterize the frequency distributions of the meteorological variables, even when all the data from different days are considered together, which may contain wind events generated by different mechanisms. Therefore, this analysis points to the usefulness of comparing weather patterns in VNOR and non-VNOR cases.

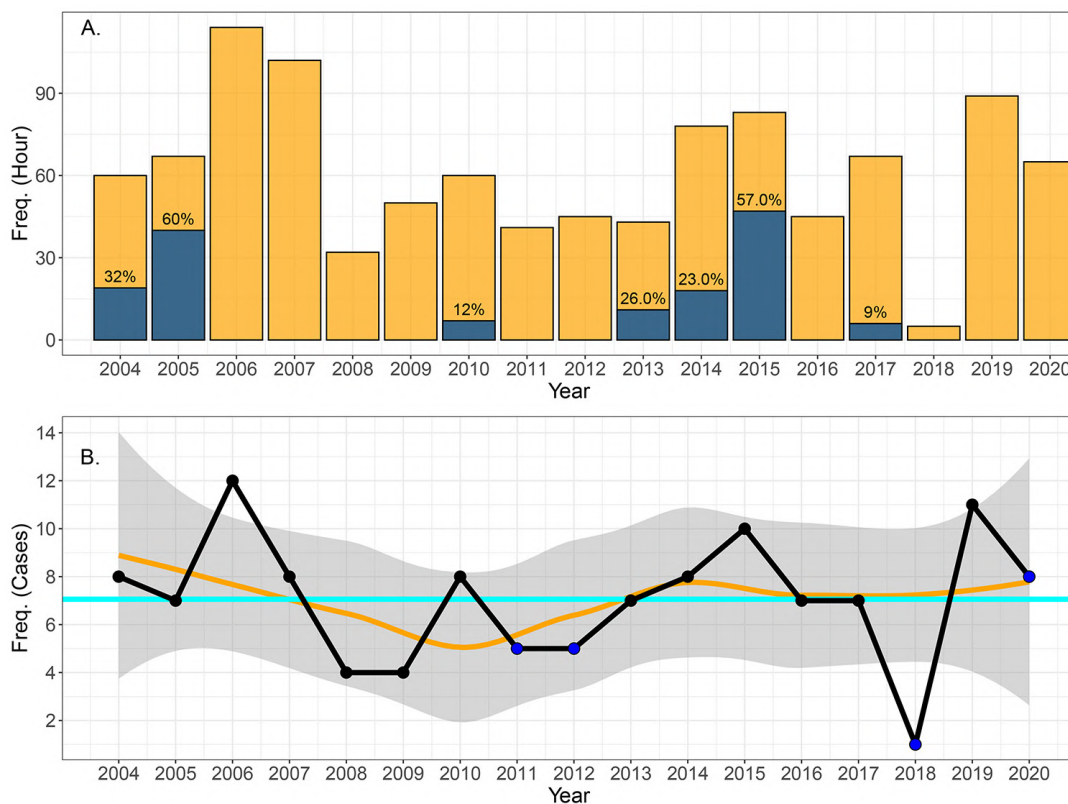


Figure 4 Data frequency: A. VNOR hours (yellow). Blue fill indicates the simultaneous occurrence of VNOR and Heat Waves; B. Cases of VNOR observed in the seventeen consecutive winters (2004–2020). Cyan line indicates the average of events, the orange line is the smoothed average with a gray margin indicating the 95% confidence level interval (linear model) and the blue dots represent the years of tower malfunction, with gaps greater than 30 days.

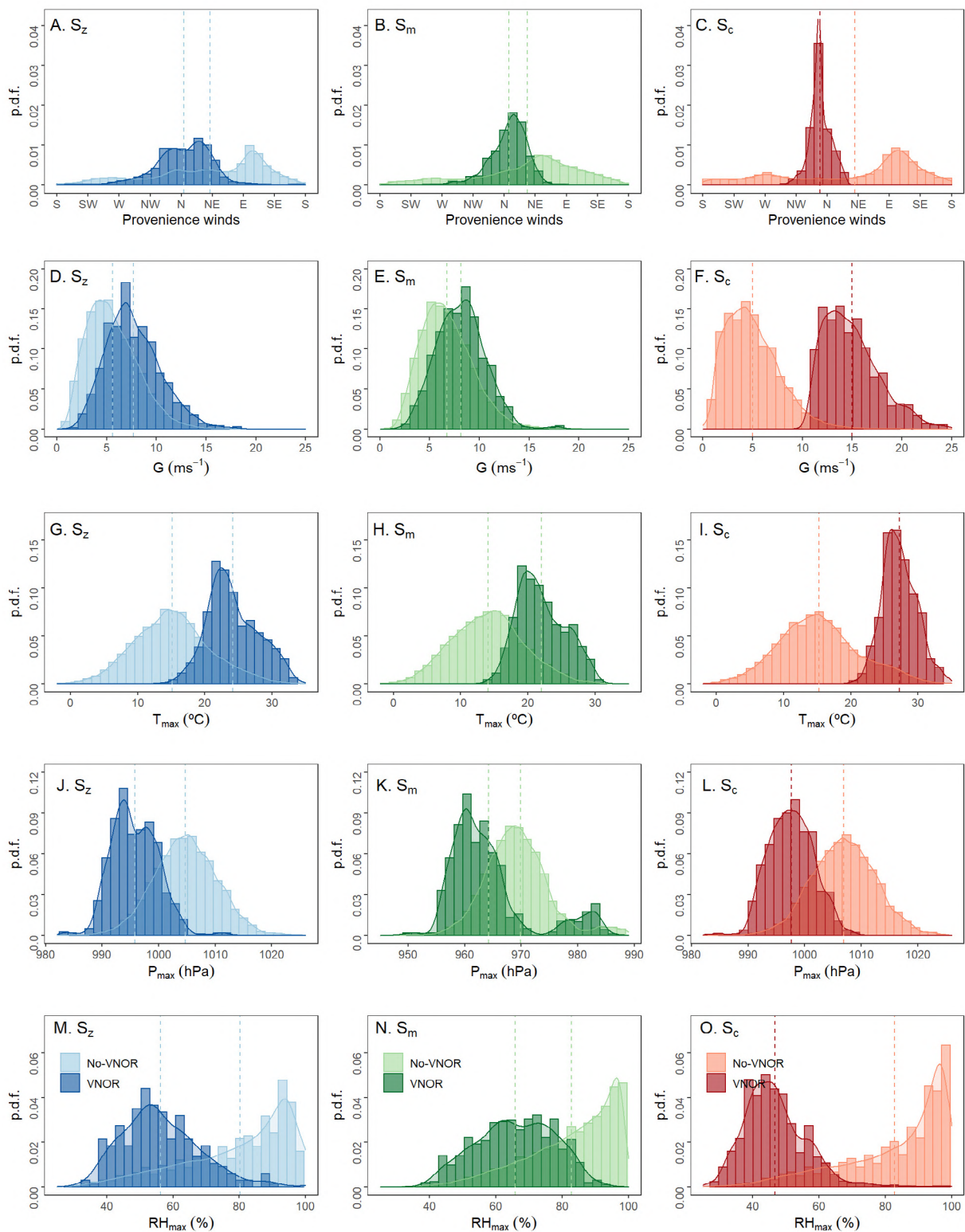


Figure 5 Probability density functions (p.d.f.): A–C. Wind direction; D–F. Wind gust (in m.s⁻¹); G–I. Maximum air temperature (in °C); J–L. Maximum atmospheric pressure (in hPa); M–O. Maximum relative humidity (in %) in the winter period from 2004 to 2020 for Sections Sz [blue], Sm [green] and Sc [red] for VNOR cases [dark color boxes] and no-VNOR cases [light color boxes]. Dashed vertical lines represent the means of the respective parameters.

In particular, during the VNOR, Sections S_c , S_m and S_z recorded a temperature increase of about 70% compared to the winter period. In addition, the average values of wind gusts from the northerly direction in Section S_c significantly increased by about 200% compared to the period without VNOR. A less significant increase in wind gusts was recorded in the S_m (28%) and S_z (41%) sections. Our findings also showed that the effects of this geophysical flow cause a decrease in atmospheric pressure in all the sectors studied and are associated with low relative humidity conditions. The average values of relative humidity during the VNOR show lower indices in Section S_c (48%) compared to those observed in Sections S_z (59%) and S_m (64%). The present analysis shows that flow characteristics are enhanced in SM (Section S_c) compared to the other regions. Such an effect seems to be provoked by local topographical features that favor this strengthening of the properties of the VNOR in the central region of RS. Thus, the analysis highlights that the VNOR phenomenon mainly influences the regional climate of southern Brazil and that its intensified features mainly occur in the central region of RS.

4 Conclusion

Large-scale synoptic conditions are responsible for developing intense airflow accelerated by local topographical effects. The development and amplification of these wind regimes depend on interactions with local surface heterogeneity. The central region of Rio Grande do Sul (RS) state has particular topographical features, with contrasting terrain elevations that can lead to topographically induced mesoscale circulations. These conditions favor developing a downslope air-flow pattern characterized by intense warm, dry winds from the northern quadrant, known as the “Vento Norte” (VNOR) phenomenon.

Based on seventeen years of meteorological observations collected by seven weather stations from INMET in southern Brazil, this study detected the occurrence of VNOR, investigated its climatological patterns in the city of Santa Maria (SM) and contrasted the main features of this phenomenon in different locations of RS.

120 VNOR episodes with an average duration of 9 h were detected throughout the winter. The year with the highest number of VNOR hours and episodes was 2006. Characteristic manifestations of the VNOR phenomenon were observed in a large region of southern Brazil. However, the different meteorological variables (i.e., temperature, wind gusts, relative humidity and atmospheric pressure) showed distinct magnitudes between Sections S_m , S_z and S_c .

The VNOR phenomenon was observed with greater intensity in the city of SM, with wind gusts that showed an average increase of 200% compared to the period without VNOR. In the other regions, the rise in this variable was more discrete, 28 and 41% in Sections S_m and S_c , respectively. Furthermore, the higher probabilities of anomalies in temperature, relative humidity, and atmospheric pressure during winter in SM were associated with strong wind gusts from the North.

Results of this study suggest that VNOR windstorm intensification in SM is influenced by a topographic forcing associated with an abrupt elevation change separating the plateau to the North from the central depression to the South of RS. In the present analysis, no regularity of occurrence was observed in the years studied. Future investigations should relate VNOR to large-scale generation systems, such as Pacific Decadal Oscillation and the El Niño-Southern Oscillation.

5 References

- Abatzoglou, J.T., Barbero, R. & Nauslar, N.J. 2013, ‘Diagnosing santa ana winds in southern California with synoptic-scale analysis’, *Weather and Forecasting*, vol. 28, no. 3, pp. 704–10, DOI:10.1175/WAF-D-13-00002.1.
- Abatzoglou, J.T., Hatchett, B.J., Fox-Hughes, P., Gershunov, A. & Nauslar, N.J. 2021, ‘Global climatology of synoptically-forced downslope winds’, *International Journal of Climatology*, vol. 41, no. 1, pp. 31–50, DOI:10.1002/joc.6607.
- Arbage, M.C.A., Degrazia, G.A., Welter, G.S., Roberti, D.R., Acevedo, O.C., de Moraes, O.L.L., Ferraz, S.T., Timm, A.U. & Moreira, V.S. 2008, ‘Turbulent statistical characteristics associated to the north wind phenomenon in southern Brazil with application to turbulent diffusion’, *Physica A: Statistical Mechanics and its Applications*, vol. 387, no. 16–17, pp. 4376–86, DOI:10.1016/j.physa.2008.02.068.
- Arrillaga, M.J., Yagüe, A.C., Román, C., Sastre, M., Jiménez, M.A., Maqueda, B.G. & Vilà-Guerau, J. 2019, ‘From weak to intense downslope winds: origin, interaction with boundary-layer turbulence and impact on CO₂ variability’, *Atmospheric chemistry and physics*, vol. 19, no. 7, pp. 4615–35, DOI:10.5194/acp-19-4615-2019.
- Ashbaugh, L.L., Malm, W.C. & Sadeh, W.Z. 1985, ‘A residence time probability analysis of sulfur concentrations at Grand Canyon National Park’, *Atmospheric Environment*, vol. 19, no. 8, pp. 1263–70, DOI:10.1016/0004-6981(85)90256-2.
- Carslaw, D.C. & Ropkins, K. 2012, ‘Openair-an R package for air quality data analysis’, *Environmental Modelling & Software*, vol. 27–28, no. 1, pp. 52–61, DOI:10.1016/j.envsoft.2011.09.008.
- Cooke, L.J., Rose, M.S. & Becker, W.J. 2000, ‘Chinook winds and migraine headache’, *Neurology*, vol. 54, no. 2, pp. 302–7, DOI:10.1212/WNL.54.2.302.

- Cruz, M.G., Alexander, M.E., Fernandes, P. M., Kilinc, M. & Sil, A. 2020, 'Evaluating the 10% wind speed rule of thumb for estimating a wildfire's forward rate of spread against an extensive independent set of observations', *Environmental Modelling & Software*, vol. 133, no. 1, pp. 104818–33, DOI:10.1016/j.envsoft.2020.104818.
- da Rosa, C.E., Stefanello, M., Facco, D.S., Roberti, D.R., Rossi, F.D., Nascimento, E.L. & Degrazia, G.A. 2022, 'Regional-scale meteorological characteristics of the Vento Norte phenomenon observed in southern Brazil', *Environmental Fluid Mechanics*, vol. 22, no. 4, pp. 819–37, DOI:10.1007/s10652-022-09855-4.
- da Rosa, C.E., Stefanello, M., Maldaner, S., Facco, D.S., Roberti, D.R., Tirabassi, T. & Degrazia, G.A. 2021a, 'Employing spectral analysis to obtain dispersion parameters in an atmospheric environment driven by a mesoscale downslope windstorm', *International Journal of Environmental Research and Public Health*, vol. 18, no. 24, pp. 13027–38, DOI:10.3390/ijerph182413027.
- da Rosa, C.E., Stefanello, M., Nascimento, E.L., Rossi, F.D., Roberti, D. R. & Degrazia, G.A. 2021b, 'Meteorological observations of the Vento Norte phenomenon in the central region of Rio Grande do Sul', *Revista Brasileira de Meteorologia*, vol. 36, no. 3, pp. 367–76, DOI:10.1590/0102-77863630141.
- dos Reis, N.C.S., Boiaski, N.T. & Ferraz, S.E.T. 2019, 'Characterization and spatial coverage of heat waves in subtropical Brazil', *Atmosphere*, vol. 10, no. 5, pp. 284–99, DOI:10.3390/atmos10050284.
- Efimov, V. & Komarovskaya, O. 2018, 'The Novaya Zemlya Bora: Analysis and numerical modeling', *Izvestiya, Atmospheric and Oceanic Physics*, vol. 54, no. 1, pp. 73–85, DOI:10.1134/S000143381801005X.
- Hang, C., Nadeau, D., Gulpepe, I., Hoch, S., Román-Cascón, C., Pryor, K., Fernando, H., Creegan, E., Leo, L., Silver, Z. & Pardyjak, E.R. 2016, 'A case study of the mechanisms modulating the evolution of valley fog', *Pure and Applied Geophysics*, vol. 173, no. 9, pp. 3011–30, DOI:10.1007/s00024-016-1370-4.
- Heldwein, A.B., Streck, N.A., Buriol, G.A., Sandri, M.A., Trentin, G., Spohr, R.B., Silva, J., Alberto, C.M. & Faria, N. 2003, 'Frequência de ocorrência de ventos fortes em Santa Maria, RS', *Revista Brasileira de Agrometeorologia*, vol. 11, no. 2, pp. 285–91.
- Iratxe, U.T. & Carslaw, D.C. 2014, 'Conditional bivariate probability function for source identification', *Environmental Modelling & Software*, vol. 59, no. 1, pp. 1–9, DOI:10.1016/j.envsoft.2014.05.002.
- Jensen, D.D., Nadeau, D.F., Hoch, S.W. & Pardyjak, E.R. 2017, 'The evolution and sensitivity of katabatic flow dynamics to external influences through the evening transition', *Quarterly Journal of the Royal Meteorological Society*, vol. 143, no. 702, pp. 423–38, DOI:10.1002/qj.2932.
- Láska, K., Chláková, Z. & Hošek, J. 2017, 'High-resolution numerical simulation of summer wind field comparing WRF boundary-layer parametrizations over complex arctic topography: case study from central spitsbergen', *Meteorologische Zeitschrift*, vol. 26, no. 4, pp. 391–408, DOI:10.1127/metz/2017/0796.
- Lehner, M., Whiteman, C.D., Hoch, S.W., Jensen, D., Pardyjak, E.R., Leo, L.S., Di Sabatino, S. & Fernando, H. J. 2015, 'A case study of the nocturnal boundary layer evolution on a slope at the foot of a desert mountain', *Journal of Applied Meteorology and Climatology*, vol. 54, no. 4, pp. 732–51, DOI:10.1175/JAMC-D-14-0223.1.
- Li, J., Sun, J., Zhou, M., Cheng, Z., Li, Q., Cao, X. & Zhang, J. 2018, 'Observational analyses of dramatic developments of a severe air pollution event in the Beijing area', *Atmospheric Chemistry and Physics*, vol. 18, no. 6, pp. 3919–35, DOI:10.5194/acp-18-3919-2018.
- Lothon, M., Lohou, F., Pino, D., Couvreur, F., Pardyjak, E., Reuder, J., Vilà-Guerau de Arellano, J., Durand, P., Hartogensis, O., Legain, D., Augustin, P., Gioli, B., Lenschow, D.H., Faloon, I., Yagüe, C., Alexander, D.C., Angevine, W.M., Bargain, E., Barrié, J., Bazile, E., Bezombes, Y., Blay-Carreras, E., van de Boer, A., Boichard, J.L., Bourdon, A., Butet, A., Campistron, B., de Coster, O., Cuxart, J., Dabas, A., Darbieu, C., Deboudt, K., Delbarre, H., Derrien, S., Flament, P., Fourmentin, M., Garai, A., Gibert, F., Graf, A., Groebner, J., Guichard, F., Jiménez, M. A., Jonassen, M., van den Kroonenberg, A., Magliulo, V., Martin, S., Martinez, D., Mastroiullo, L., Moene, A.F., Molinos, F., Moulin, E., Pietersen, H. P., Piguet, B., Pique, E., Román-Cascón, C., Rufin-Soler, C., Saïd, F., Sastre-Marugán, M., Seity, Y., Steeneveld, G.J., Toscano, P., Traullé, O., Tzanos, D., Wacker, S., Wildmann, N. & Zaldei, A. 2014, 'The bllast field experiment: boundary-layer late afternoon and sunset turbulence', *Atmospheric chemistry and physics*, vol. 14, no. 20, pp. 10931–60, DOI:10.5194/acp-14-10931-2014.
- MacDonald, M.K., Pomeroy, J.W. & Essery, R.L. 2018, 'Water and energy fluxes over northern prairies as affected by chinook winds and winter precipitation', *Agricultural and Forest Meteorology*, vol. 248, no. 1, pp. 372–85, DOI:10.1016/j.agrformet.2017.10.025.
- Mass, C.F. & Ovens, D. 2019, 'The northern California wildfires of 8–9 October 2017: The role of a major downslope wind event', *Bulletin of the American Meteorological Society*, vol. 100, no. 2, pp. 235–56, DOI:10.1175/BAMS-D-18-0037.1.
- Math, F.A. 1934, 'Battle of the chinook wind at Havre, mont', *Monthly Weather Review*, vol. 62, no. 2, pp. 54–7, DOI:10.1175/1520-0493(1934)62<54:BOTCWA>2.0.CO;2.
- Moore, G. 2013, 'The Novaya Zemlya bora and its impact on Barents sea air-sea interaction', *Geophysical research letters*, vol. 40, no. 13, pp. 3462–67, DOI:10.1002/grl.50641.
- Nascimento, E.D.L. & Chamis, M.L. 2012, 'Atmospheric conditions associated with the windstorm "vento norte"', in *Croatia-USA Workshop on Mesometeorology*, Zagreb, pp. 32-3, viewed 03 November 2022, <https://www.pmf.unizg.hr/_download/repository/2_Collection_Participant_Abstacts%5B2%5D.pdf>.
- Norte, F.A. 2015, 'Understanding and Forecasting Zonda Wind (Andean Foehn) in Argentina: A Review', *Atmospheric and Climate Sciences*, vol. 5, no. 3, pp. 163–93, DOI:10.4236/acs.2015.53012.
- Otero, F. & Araneo, D. 2021, 'Zonda wind classification using machine learning algorithms', *International Journal of Climatology*, vol. 41, no. S1, pp. 342–53, DOI:10.1002/joc.6688.

- Pereira, H.R., Reboita, M.S. & Ambrizzi, T. 2017, 'Características da atmosfera na primavera austral durante o El Niño de 2015/2016', *Revista Brasileira de Meteorologia*, vol. 32, no. 2, pp. 293–310, DOI:10.1590/0102-77863220011.
- Raphael, M. 2003, 'The Santa Ana winds of California', *Earth Interactions*, vol. 7, no. 8, pp. 1–13, DOI:10.1175/1087-3562(2003)007%3C0001:TSAWOC%3E2.0.CO;2.
- Richner, H. & Hächler, P. 2013, 'Understanding and forecasting Alpine Foehn', in F. Chow, S. de Wekker & B. Snyder (eds), *Mountain Weather Research and Forecasting: Recent Progress and Current Challenges*, Springer, Dordrecht, pp. 219–60, DOI:10.1007/978-94-007-4098-3_4.
- Román-Cascón, C., Yagüe, C., Mahrt, L., Sastre, M., Steeneveld, G.-J., Pardyjak, E., Boer, A. & Hartogensis, O. 2015, 'Interactions among drainage flows, gravity waves and turbulence: a blast case study', *Atmospheric Chemistry and Physics*, vol. 15, no. 15, pp. 9031–47, DOI:10.5194/acp-15-9031-2015.
- Samuelsen, E.M. & Graversen, R.G. 2019, 'Weather situation during observed ship-icing events off the coast of northern Norway and the Svalbard archipelago', *Weather and Climate Extremes*, vol. 24, no. 1, e100200, DOI:10.1016/j.wace.2019.100200.
- Sartori, M.G.B. 2003, 'Gênese e características do vento norte regional em Santa Maria/RS', *X Simpósio brasileiro de geografia física e aplicada*, Universidade do Estado do Rio de Janeiro, Rio de Janeiro, viewed 03 November 2022, <<http://www.cibergeo.org/XSBGFA/eixo3/3.2/286/286.htm>>.
- Sartori, M.G.B. 2016, *O Vento Norte*, DR Publicidade Editora, Santa Maria.
- Shestakova, A. & Moiseenko, K. 2018, 'Hydraulic regimes of flow over mountains during severe downslope windstorms: Novorossiysk bora, Novaya Zemlya bora, and Pevék Yuzhak', *Izvestiya, Atmospheric and Oceanic Physics*, vol. 54, no. 4, pp. 344–53, DOI:10.1134/S0001433818040291.
- Shestakova, A., Toropov, P.A. & Matveeva, T.A. 2020, 'Climatology of extreme downslope windstorms in the Russian Arctic', *Weather and Climate Extremes*, vol. 28, no. 1, e100256, DOI:10.1016/j.wace.2020.100256.
- Smith, C., Hatchett, B.J. & Kaplan, M. 2018, 'A surface observation based climatology of diablo-like winds in California's wine country and western Sierra Nevada', *Fire*, vol. 1, no. 2, pp. 1–9, DOI:10.3390/fire1020025.
- Stefanello, M., de Lima Nascimento, E., da Rosa, C.E., Degrazia, G., Mortarini, L. & Cava, D. 2020, 'A micrometeorological analysis of the vento norte phenomenon in southern Brazil', *Boundary-Layer Meteorology*, vol. 176, no. 3, pp. 415–39, DOI:10.1007/s10546-020-00540-x.
- Sun, H., Clark, T.L., Stull, R.B. & Black, T.A. 2006, 'Two-dimensional simulation of airflow and carbon dioxide transport over a forested mountain: Part ii. carbon dioxide budget analysis and advection effects', *Agricultural and forest meteorology*, vol. 140, no. 1, pp. 352–64, DOI:10.1016/j.agrformet.2006.03.016.
- USGS - United States Geological Survey, Earth Resources Observation and Science (EROS) Center 2022, *USGS EROS Archive - Digital Elevation - Shuttle Radar Topography Mission (SRTM) Non-Void Filled*, viewed 10 October 2022, <<https://www.usgs.gov/centers/eros/science/usgs-eros-archive-digital-elevation-shuttle-radar-topography-mission-srtm-non-void-filled>>.
- Wang, W., Zhou, W., Li, X., Wang, X. & Wang, D. 2016, 'Synoptic-scale characteristics and atmospheric controls of summer heat waves in China', *Climate dynamics*, vol. 46, no. 9, pp. 2923–41, DOI:10.1007/s00382-015-2741-8.
- Whiteman, C.D. 1982, 'Breakup of temperature inversions in deep mountain valleys: Part i. observations', *Journal of Applied Meteorology and Climatology*, vol. 21, no. 3, pp. 270–89, DOI:10.1175/1520-0450(1982)021%3C0270:BOTIID%3E2.0.CO;2.
- Würsch, M. & Sprenger, M. 2015, 'Swiss and Austrian foehn revisited: A lagrangian-based analysis', *Meteorologische Zeitschrift*, vol. 24, no. 3, pp. 225–42, DOI:10.1127/metz/2015/0647.

Author contributions

Cinara Ewerling da Rosa: conceptualization; formal analysis, methodology; validation; writing – original draft; writing review and editing; visualization. **Michel Stefanello:** conceptualization; formal analysis, methodology; validation; writing – original draft; writing review and editing; visualization. **Douglas Stefanello Facco:** writing review and editing; visualization. **Débora Regina Roberti:** funding acquisition; supervision. **Fábio Diniz Rossi:** writing – original draft; writing review and editing; visualization. **Gervásio Annes Degrazia:** conceptualization; writing – original draft; writing review and editing; visualization; supervision.

Conflict of interest

The authors declare no potential conflict of interest.

How to cite:

da Rosa, C.E., Stefanello, M., Facco, D.S., Roberti, D.R., Rossi, F.D. & Degrazia, G.A. 2023, 'Climatological Features of the Vento Norte Phenomenon in the Extreme South of Brazil', *Anuário do Instituto de Geociências*, 46:52599. https://doi.org/10.11137/1982-3908_2023_46_52599

Data availability statement

All data included in this study are publicly available in the literature.

Funding information

Not applicable.

Editor-in-chief

Dr. Claudine Dereczynski

Associate Editor

Dr. Fernanda Cerqueira Vasconcellos